


Evaluation of Automatic Emergency Braking Systems in Two-Wheeler Crash Scenarios

Transportation Research Record
2023, Vol. 2677(9) 175–187
© National Academy of Sciences:
Transportation Research Board 2023
Article reuse guidelines:
sagepub.com/journals-permissions
DOI: 10.1177/03611981231158637
journals.sagepub.com/home/trr


Weixuan Zhou^{1,2}  and Xuesong Wang^{1,2} 

Abstract

The two-wheeler (TW) is a popular means of transportation in China, but TWs often suffer from serious traffic crashes because of their highly flexible trajectory and low detectability. Therefore, they present a challenge for the sensing and decision-making systems in autonomous vehicles (AVs). Collision avoidance systems, such as automatic emergency braking (AEB), have provided an effective way for AVs to avoid collisions with different objects, including TWs. The effectiveness of the AEB system is highly dependent on its parameter configurations, however, which vary among TW crash scenarios. This study, therefore, evaluates the AEB parameters, including time to collision (TTC), deceleration, and detection area (including detection range, field of vision, and trigger width) in two AEB systems: one-stage AEB and three-stage AEB. A total of 243 crashes extracted from the China In-Depth Accident Study database were simulated in Matlab's Simulink. Results show: (i) one-stage AEB crash avoidance rates range from 15.2% to 81.5%, while three-stage AEB has crash avoidance rates as high as 87.2%; (ii) deceleration, TTC, and detection area all have significant main effects on crash rate, but detection area has less influence in longitudinal than in crossing scenarios; (iii) higher crash avoidance rates resulted in lower traffic efficiency for both AEB systems, but resulted in greater speed reduction only for one-stage AEB; and (iv) collisions are less likely to be avoided in scenarios with high initial speed of TW and AV. This study demonstrates the performance of AEB algorithms in multiple actual crash scenarios and provides a reliable basis for the development of AEB systems.

Keywords

China In-depth Accident Study (CIDAS), two-wheeler crashes, crash scenarios, automatic emergency braking (AEB), simulation

Two-wheelers (TWs), which in this paper refers to bicycles and e-bikes but not motorcycles, are commonly used for commuting and delivering goods in China because of their low cost and convenience. It is estimated that China has the largest number of TWs in the world, with nearly 400 million bicycles and 300 million e-bikes (1), and they have high crash rates. In 2019, TWs represented 22.16% of road traffic fatalities in China (2), while in the UK (3) and Australia (4) rates are only 6% and 3%, respectively. In other Asian countries, the proportion of fatal crashes involving TWs is even higher than in China, with around 60%–70% of road traffic fatalities (5). Europe, too, is starting to experience an increase in TW fatalities because of the rapid increase in e-bike ownership. For example, Sweden had a 10% increase in powered-TW road fatalities from 2000 to 2018, a period in which the total number of road fatalities decreased significantly (6). With the popularization

of autonomous vehicles (AVs), the sensors and decision-making systems of AVs must cope with the challenge of preventing crashes with TWs arising from their variety of appearance and their unpredictable trajectories.

Automatic emergency braking (AEB), also known as autonomous emergency braking, is a collision avoidance system designed to help drivers avoid or mitigate the severity of crashes in SAE level 2 AVs. With front radar and cameras detecting the position and velocity of surrounding objects, AEB can work with forward collision warning (FCW) (7, 8) systems to alert drivers of

¹School of Transportation Engineering, Tongji University, Shanghai, China

²The Key Laboratory of Road and Traffic Engineering, Ministry of Education, Shanghai, China

Corresponding Author:

Xuesong Wang, wangxs@tongji.edu.cn

potential risk, and automatically apply brake support or emergency braking when the vehicle is on the verge of collision. AEB has been demonstrated to be effective in avoiding collisions, and in reducing speed when collisions cannot be avoided (9, 10). Consequently, the European Commission and the United States have issued laws and regulations requiring the installation of AEB and FCW in new cars and trucks (11, 12). To adapt AEB to the characteristics of cyclists, an AEB cyclist system was developed by SafetyCube DSS, the European Road Safety Decision Support System (13). Car assessment organizations, such as Euro NCAP (New Car Assessment Programme), C-NCAP, and C-IASI (China Insurance Automotive Safety Index), have developed protocols and test scenarios for cyclists because of the growing concern for cyclist safety. AEB systems differ from one another, however, and to the best of the authors' knowledge, though many studies have focused on the effectiveness of AEB cyclist systems, few have compared the performance of AEB systems with different braking patterns, such as one-stage and three-stage, in cyclist crashes.

The effectiveness of an AEB system is significantly influenced by the values of its parameters, such as time to collision (TTC), deceleration, field of view (FoV), detection range, and trigger width. The TTC value determines AEB activation time and is the key factor influencing the rates of false and missing alarms (14–16). A larger FoV and detection range can cover a wider detection area, which is thus able to avoid more crashes (17), an important consideration in TW safety because Lenard et al. (18) found that cyclists scatter laterally even more widely than pedestrians. However, a large detection area requires more costly high-technology sensors, which may not be necessary for all types of scenarios, as Char et al. (19) found that FoV has little influence on crash rate in longitudinal scenarios. A large deceleration will offer an even greater benefit than increasing FoV (20), but will reduce the occupants' comfort (21). To determine optimal parameters, it is therefore necessary to evaluate the AEB parameters in different scenarios.

To reconstruct scenarios for testing, previous studies have collected data recorded from taxi driving and naturalistic driving data (21–23). The position and velocity of cyclist and car can be easily obtained from the recorder output, making the reconstruction convenient. However, in both types of database, the probability of drivers encountering crashes is low (24), so collecting enough data is difficult. In-depth crash databases are another commonly used way to create pre-crash scenarios based on on-site investigation and crash reconstruction. The first crash research team was the Volvo Accident Research Team founded in 1969 arising from the need for knowledge on the causes of crashes (25).

The German In-Depth Accident Study (GIDAS) was initiated in 1999; it is the largest in-depth accident study project in Germany, and continues to record approximately 2,000 crashes annually (26). In 2011, the China In-Depth Accident Study (CIDAS) was initiated and has recorded more than 7,000 crashes to date, which is an abundance of data for analyzing TW crashes.

The objective of this study is to determine the AEB parameters that will result in optimal safety for the vulnerable TW in the AV traffic environment. This study will therefore cluster and reconstruct various crash scenarios between TW and passenger cars to explore the influence of different AEB parameters and systems on crash avoidance and mitigation rates. The two selected AEB systems are one-stage AEB and three-stage AEB, which represent the most commonly used AEB systems. Correlations between crash avoidance rate and factors such as traffic efficiency, speed reduction, and TW and motor vehicle speed are considered.

Literature Review

Safety System Assessing Approach

There are two main approaches to studying the performance of safety systems: retrospective and prospective. A retrospective study assesses the safety performance of a new system or function by comparing the number of real-life crashes of vehicles with and without the system (13). This approach uses data collected on roadways and can provide reliable results, but the typically limited sample size of vehicles equipped with the system to be tested means that results have not always been statistically significant (27). A prospective study is used to assess the effectiveness of a safety system before its practical application, or when there is not enough real-life data (28). Much of this research uses counterfactual simulation to assess the performance of active safety systems with reconstructed crash scenarios (29–32). In a counterfactual simulation, the crashes are simulated in a virtual environment, and compared with the effects of simulations using an active safety system, in which various scenarios and system parameters can be fully and repeatedly tested. Though the authenticity of counterfactual simulation is lower than retrospective studies, its low cost makes it an efficient approach for assessing active safety systems.

Test Scenario Generation

Crash scenarios can be generated based on the trajectory and relative position of the two crash participants. Kuehn et al. (33) clustered cyclists' trajectory relative to the car into right, left, head-on, and same, and generated four different scenarios. In the CATS (Cyclist-AEB

Testing System) project, scenarios were defined by the orientation of the cyclist with respect to the car, as well as the trajectories of both participants, and five types of scenarios with 12 divisions were defined (34). The AsPeCSS (Assessment methodologies for forward looking integrated pedestrian and further extension to cyclist safety systems) project applied a similar approach as CATS and generated four scenarios for testing (35). Clustering methods such as K-means, K-medoids and hierarchical clustering (29, 36, 37) have also been widely used to develop car-to-TW test scenarios. Despite different clustering methods, the essential variables that play decisive roles are consistent: motion of the car, motion of the TW, and the relative motion direction between the car and TW.

Autonomous Emergency Braking

AEB systems that have been tested and are currently in the marketplace can be classified into at least three categories: (i) one-stage AEB, activated by a time-related trigger such as TTC or a distance-related trigger such as safe braking distance, (ii) AEB combined with FCW, and (iii) multi-stage AEB with or without FCW (10, 38). The most fundamental and commonly used collision avoidance pattern is one-stage AEB activated by TTC (39). In this AEB system, when the TTC drops below a pre-defined value (usually between 0.5 s and 1.5 s), the vehicle automatically performs an emergency braking maneuver. The addition of multiple stages and FCW is intended to assist drivers better by giving them enough time to perform a proper evasive maneuver, and then to provide full braking when a crash becomes otherwise unavoidable (40). Some manufacturers, such as Audi, Volvo, and Volkswagen, combine FCW with multi-stage partial and fully autonomous braking. The three-stage AEB used in the Audi A7 has been tested and shown to perform well (40), as has the basic and commonly used one-stage AEB (17, 22).

Data Preparation

Data Extraction from CIDAS

CIDAS is a database that contains detailed information about traffic crashes that involve at least one four-wheel motor vehicle and cause road user injury. The continuing data collection effort is conducted by the China Automotive Technology and Research Center (CATARC), which has recorded more than 7,000 cases since 2011. Professional investigation teams collect more than 3,000 variables per case, including crash type, vehicle damage, crash causation, injuries, road infrastructure, traffic, and environment. In addition to conducting on-site investigations, surveillance videos and videos filmed

by drones are processed to build the CIDAS Pre-Crash Database, in which the road alignments, markings and signs of the crash location, and trajectories of the crash participants are reconstructed from 5 s before the crash up to the moment of the crash.

This study uses CIDAS data collected between 2019 and 2021. A total of 1,580 crashes were recorded in the dataset. Restricting the count to crashes involving two participants, a TW and a four-wheel passenger car (also referred to as the vehicle, or SV for subject vehicle), the number decreased to 432. In this study, TW includes bicycles and electric bikes as they have similar characteristics and share bicycle lanes, although electric bikes usually have higher speeds. Motorcycles are excluded from this study. Vehicle speed was omitted from the data collected on two of the crashes, making it impossible to fully reconstruct the pre-crash scenarios; therefore, 430 crashes were extracted as the sample for analysis.

Clustering and Analysis of the Scenarios

Four basic scenario types were defined by SV trajectory and the relative orientation of the TW with respect to the SV: crossing (C) at 45.12% of the 430 crashes; turning (T) at 36.05%; longitudinal (L) at 12.33%; and on-coming (On) at 2.09%. A few additional events in which the SV was parking or backing up were classified as remaining (Re), representing 4.42% of the 430 crashes.

The characteristics of all five types of scenarios were analyzed, including TW rider injury, view obstruction of TW and SV, and initial speed and collision speed of TW and SV. The Abbreviated Injury Scale (AIS) ranks injury severity on a six-point scale (1 = minor, 6 = maximal) (41). As is shown in Figure 1a, fatal and serious injury (AIS3 +) rates for TW riders in crossing scenarios were 21.1% and 25.3%, respectively, and together accounted for 28.3% of longitudinal crashes, while the majority of the turning crashes resulted in only minor injury (AIS1 and AIS2). On-coming and remaining scenarios both showed high fatal and severe injury rates, but the sample sizes of these two scenarios are small. As is shown in Figure 1b, view obstruction is a common characteristic, with views obstructed mostly by buildings or by parking or moving vehicles. In 35.8% of the crossing scenarios, the view of the TW rider, the SV driver, or both is obstructed, which makes it not only difficult for them to avoid crashes, but also presents a great challenge for AV sensor detection. As is shown in Figure 1, c and d, the mean initial speed of SVs is 45.9 km/h and their mean speed at the time of collision is 40.6 km/h, with a 5.3 km/h speed reduction on average. The mean initial and collision speed of TWs is 21.0 km/h and 20.4 km/h, with only a 0.6 km/h speed reduction.

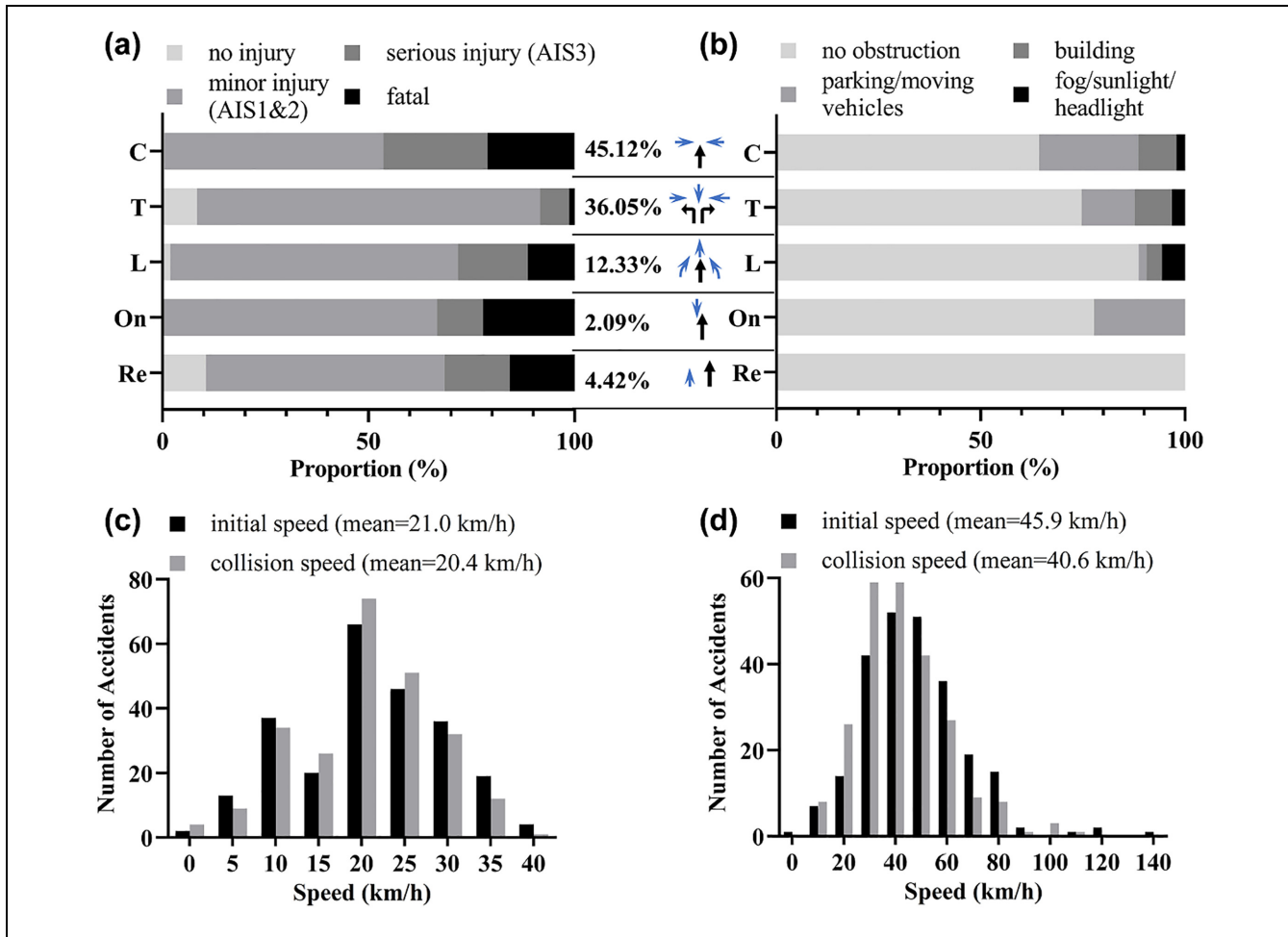


Figure 1. Characteristics of the five scenarios: (a) two-wheeler rider injury, (b) view obstruction, (c) initial and collision speed of two-wheeler, and (d) initial and collision speed of subject vehicle.

Test Scenario Generation

As crossing and longitudinal scenarios both have high injury severity and adequate sample sizes, these two scenario types are used to test the AEB parameters, thus reducing the total studied crashes to 243. The two scenario types are further divided into seven scenarios based on the TW maneuver, as is shown in Figure 2.

Scenario types C1–C4 are crossing scenarios. In C1 and C2, SV is driving straight and TW crosses from either the left or right side of the vehicle. View obstruction was observed in 41.9% and 39.2% of these two scenarios, respectively. Since obstruction was mostly by physical objects such as parked or moving vehicles, two parked cars are illustrated in Figure 2 in the lanes adjacent to the SV to represent the obstructions close to the collision point. TW's trajectory is perpendicular to SV's trajectory and 3 m from the road boundary, the 3 m representing the typical sidewalks and road shoulders. In C3 and C4, both illustrated in the third image, TW first travels straight in

either the same direction as SV or the opposite direction, after which it makes an approximately 90-degree turn in front of the SV, which results in a crash. In the fourth image, L1–L3 are longitudinal scenarios in which SV and TW travel in the same direction, usually sharing the same lane or traveling on roads without bicycle lane separators. The crashes are mostly caused by the misoperation or distraction of either SV or TW driver. In L1, TW travels in front of SV and they both follow a straight trajectory; TW is rear-ended by SV. In L2 and L3, TW travels in the same direction as SV in an adjacent lane, after which TW unexpectedly swerves in front of SV and their trajectories coincide at the collision point.

Methodology

Simulation Platform

This study used the Matlab Automatic Driving Toolbox to create the driving scenarios and to simulate driving

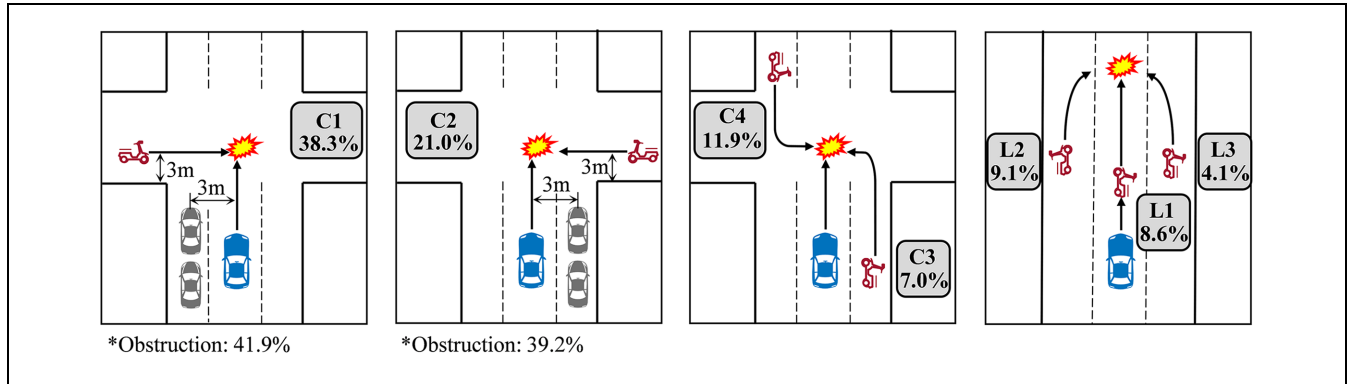


Figure 2. Test scenarios.

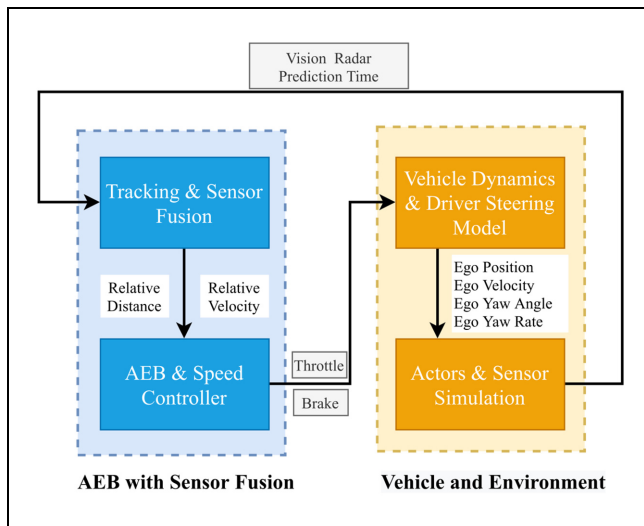


Figure 3. Automatic emergency braking (AEB) simulation procedure in Simulink.

behavior under the AEB systems. MATLAB's Driving Scenario Designer app was used to create the test scenario for every crash, with the inputs of the road's center and width, the TW's trajectory and velocity, and the initial velocity and position of the SV, now the simulated AV, or ego car. The simulation was realized by the collaboration of two subsystems consisting of four blocks. Figure 3 illustrates the blocks designed in Simulink to test the AEB system.

In the AEB with Sensor Fusion subsystem, the tracking and sensor fusion block fuses the data from the sensors and detects the most important object (MIO), as well as its position and velocity. The AEB and speed controller decides the driving strategy of the next simulation step by analyzing the current safety condition, and outputs the brake pressure or throttle to the Vehicle and Environment subsystem. The vehicle dynamics and driver steering model block models the dynamics of the

simulated ego car as it drives along the road. As the focus of this study is on braking systems, no steering maneuver is applied. The motion of the ego car is synchronized in the scenario by the actors and sensor simulation block, after which the sensors output the data for the next step in the simulation.

The velocity and trajectory of TWs from 5 s before the collision up to 1 s after the potential collision point were generated using TW initial and collision speeds extracted from the crash data, as well as their trajectories according to the crossing and longitudinal scenarios shown in Figure 2. For each scenario, the SV travels at a constant initial speed from its origin coordinates until the braking is triggered, whereupon one of the tested AEB systems will take control of the SV's speed.

AEB Systems

Two different AEB systems—a one-stage AEB system and a three-stage AEB system—were studied for comparison. The two AEB systems activate and take control of the braking system if the following criteria are met (Figure 4a):

- the TW is inside the detection range and sensor FoV so that its position and speed can be obtained by the sensor;
- the TW is inside the trigger width (w), so that only road users that are likely to influence the ego car are considered, avoiding unnecessary activations from road users far away from the driving path;
- predicted TTC is shorter than the TTC threshold of one-stage AEB and shorter than the calculated stopping time of three-stage AEB (Figure 4b).

In the one-stage AEB system modeled in this study, the vehicle brakes with a constant deceleration dec when the TTC is shorter than a pre-defined threshold, as illustrated in Figure 4b. Three-stage AEB utilizes a different

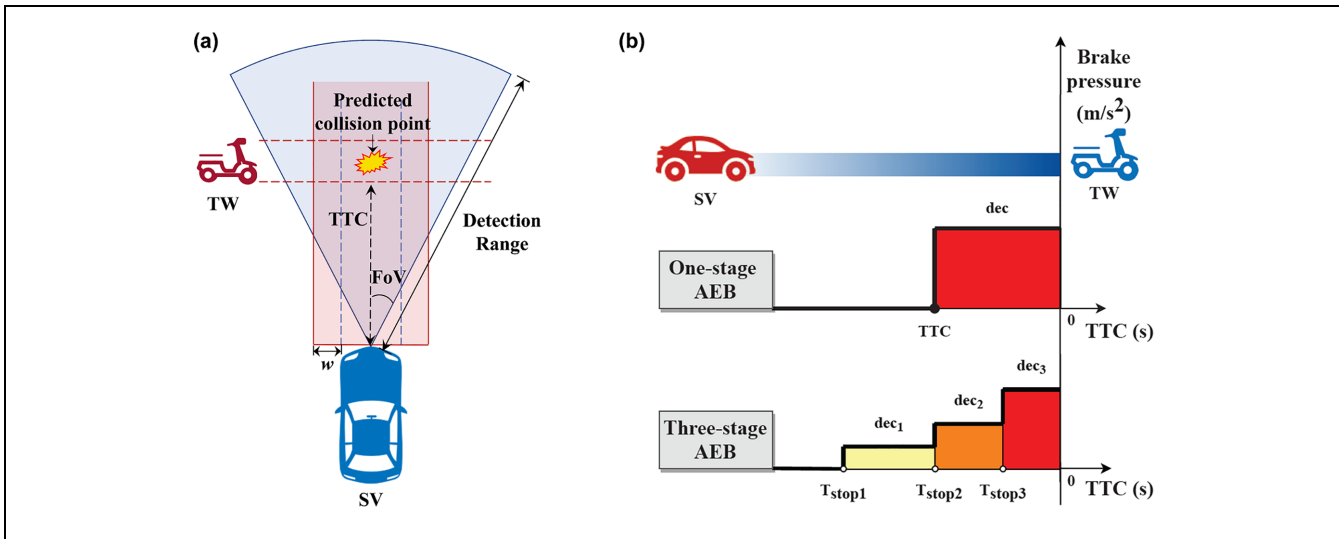


Figure 4. Basis for automatic emergency braking (AEB) systems: (a) parameters for decision making and (b) braking profiles of AEB systems.

Table 1. Parameters Used in Existing Cyclist Collision Avoidance System Research

Author	Time to collision (s)	Deceleration (g)	Field of view (°)	w (m)	Detection range (m)
Peng et al. (21)	[1.0-2.0]	[0.6, 0.8]	[20, 90]	NA	NA
Jeppsson and Lubbe (20)	0.7	0.9, 1.8	37.5, 90	1.2	[0, 60]
Rosen (17)	0.5, 1.0, 1.5	0.5, 0.7, 0.9	20, 45	0, 1.0, 5.0	[7, 60]
Zhao et al. (30)	1.4	0.5, 0.8	25, 45, 180	NA	70
Chajmowicz et al. (42)	1	0.9	18, 60, 90	NA	[20, 70]
Char et al. (19)	NA	NA	30, 50, 70	NA	50
Char and Serre (43)	NA	0.82	[10, 70]	NA	[5, 45]

Note: NA indicates that the parameter is not available.

stopping time calculation approach, which continuously compares current TTC with stopping time. Stopping time is a parameter that varies with speed and is defined as the time from when the ego vehicle first applies its brake a_{brake} to the time it comes to a complete stop:

$$\tau_{stop} = \frac{v_{ego}}{a_{brake}} \quad (1)$$

As shown in Figure 4b, the three-stage AEB brake process is divided into three stages that are triggered depending on the urgency of the driving condition, during which three different brake pressures, dec_1 , dec_2 , and dec_3 , are applied. The stopping time at each braking stage (T_{stop1} , T_{stop2} , T_{stop3}) is calculated, whereupon if TTC is shorter than stopping time, brake pressure is applied.

Parameters

The parameters that are necessary for the two AEB systems include TTC, deceleration, FoV, sensor detection

range, and trigger width (w). A summary of these parameters as used in existing research on cyclist collision avoidance systems is shown in Table 1.

The specific values of the parameters in this study are listed in Table 2. They were chosen based on the existing research for the following reasons:

- The TTC threshold to trigger braking in existing research is around 1.0 s, and seldom exceeds 2.0 s, as a long TTC will lead to a high false alarm rate with unexpected interruptions to the driver (16). Therefore, three TTC values, 0.5 s, 1.0 s, and 1.5 s, were chosen for comparison of one-stage AEB systems. As discussed, three-stage AEB does not use a TTC threshold.
- Vehicle deceleration varies between 0.5 g and 0.9 g in most of the research. A deceleration higher than 1.0 g, as Jeppsson et al. (20) applied to test vacuum emergency braking with a special vacuum pad technique, can hardly be achieved by common vehicles nor applied in tests. Three deceleration

Table 2. Automatic Emergency Braking (AEB) Parameters Under Study

One-stage AEB								
ID	dec (g)	ID	dec (g)	ID	dec (g)	TTC (s)	FoV (°)	w (m)
1AEB-1	0.9	1AEB-7	0.7	1AEB-13	0.5	1.5	80	5
1AEB-2		1AEB-8		1AEB-14			40	1
1AEB-3		1AEB-9		1AEB-15		1	80	5
1AEB-4		1AEB-10		1AEB-16			40	1
1AEB-5		1AEB-11		1AEB-17		0.5	80	5
1AEB-6		1AEB-12		1AEB-18			40	1
Three-stage AEB								
ID	dec ₁ (g)	dec ₂ (g)	dec ₃ (g)	FoV (°)	w (m)			
3AEB-1	0.5	0.7	0.9	80	5			
3AEB-2	0.5	0.7	0.9	40	1			

Note: dec = deceleration; FoV = field of view; TTC = time to collision; w = trigger width. Each group of three one-stage AEB algorithms sharing the same row (for example, 1AEB-1, 1AEB-7, and 1AEB-13) has the same TTC, FoV, and w.

values were chosen in this study, 0.5 g, 0.7 g, and 0.9 g for the three-stage AEB system, and for comparison of one-stage AEB systems.

- Different definitions of FoV appear in existing research. FoV can indicate either the sensor's total detection field (17, 30) or half of the detection field (19, 43). In this study, FoV follows the latter definition; therefore, an FoV of 20° corresponds to a total detection field of 40°. Lenard et al. (18) found that an FoV of $\pm 80^\circ$ can detect 90% of cyclists, so a radar FoV of 80° was applied in this study, and a smaller FoV of 40° was chosen for comparison.
- Rosen et al. (17) considered cyclist travel speed as the main factor determining AEB trigger width and chose 5.0 m as the maximum width, which is the distance a cyclist travels in 0.9 s at a speed of 20 km/h. The average speed of TW riders is around 20 km/h in our samples, so a maximum width of 5.0 m was chosen. A minimum trigger width of 1.0 m was chosen to limit the influence area of the surrounding vehicles to within the ego vehicle's lane.
- The detection range in this study is a fixed value of 70 m, following the maximum detection range in the existing research.

Table 2 shows the three values that were chosen for both TTC and deceleration. FoV and trigger width were combined into two groups of detection area: FoV = 80° with $w = 5$ m (wide detection area) and FoV = 40° with $w = 1$ m (narrow detection area). For $w = 5$ m, in many cases the trigger width may be outside of the FoV = 40°; conversely, for $w = 1$ m, in most cases FoV = 80° would waste detection resources. Therefore, these two combinations were not tested. As is shown in Table 2, a total of 18 groups of parameters were tested for the one-stage AEB

system, resulting in 18 different one-stage AEB algorithms (1AEB-1 through 1AEB-18) with the same decision logic but different parameters. For three-stage AEB, the three stages of dec_1 , dec_2 , and dec_3 were set as 0.5 g, 0.7 g, and 0.9 g, respectively, and were tested with two groups (3AEB-1, 3AEB-2) of FoV and trigger width.

Results and Analysis

Crash Avoidance and Mitigation Rates

The overall performance of the 18 one-stage AEB systems and two three-stage AEB systems, which vary in combinations of deceleration, TTC, and detection area (FoV and trigger width are considered together), were evaluated for crash avoidance rate and mitigation rate. Crash avoidance rate is the number of avoided crashes divided by the total number of crashes (243 in this study). For crashes that were not avoided by AEB, if the ego vehicle's speed at the time of collision speed is lower than its initial speed, crash severity is considered to be mitigated, therefore, crash mitigation rate is the number of mitigated crashes divided by the total number of crashes. In every simulated case, the ego vehicle's sensor detected the TW and successfully activated AEB before the collision, even if the collision was not avoided; therefore, the crash mitigation rate is one minus the crash avoidance rate. For example, a system in this study with a crash avoidance rate of 81.5% has a mitigation rate of 18.5%.

Figure 5 illustrates the crash avoidance and crash mitigation rates of the one-stage AEB and three-stage AEB algorithms. The crash avoidance rates of the one-stage AEB algorithms range from 15.2% (1AEB-18) to 81.5% (1AEB-1), with the average avoidance rate of 40.9%. The two three-stage AEB algorithms 3AEB-1 and 3AEB-2 have crash avoidance rates of 87.2% and 51.9%, respectively.

Table 3. Post-Hoc Analysis of One-Stage Automatic Emergency Braking (AEB) Crash Avoidance Rates by Scenario Type

Scenario	Paired condition of parameters						
	Deceleration			Time to collision			Detection area
	0.9 and 0.7	0.9 and 0.5	0.7 and 0.5	1.5 and 1.0	1.5 and 0.5	1.0 and 0.5	Wide and narrow
All							
Difference	0.088	0.192	0.104	0.110	0.349	0.239	0.126
p-value	< 0.001	< 0.001	< 0.001	< 0.001	< 0.001	< 0.001	< 0.001
Crossing							
Difference	0.090	0.195	0.104	0.073	0.244	0.171	0.150
p-value	< 0.001	< 0.001	< 0.001	< 0.001	< 0.001	< 0.001	< 0.001
Longitudinal							
Difference	0.079	0.182	0.104	0.242	0.726	0.484	0.040
p-value	0.002	< 0.001	< 0.001	< 0.001	< 0.001	< 0.001	0.050

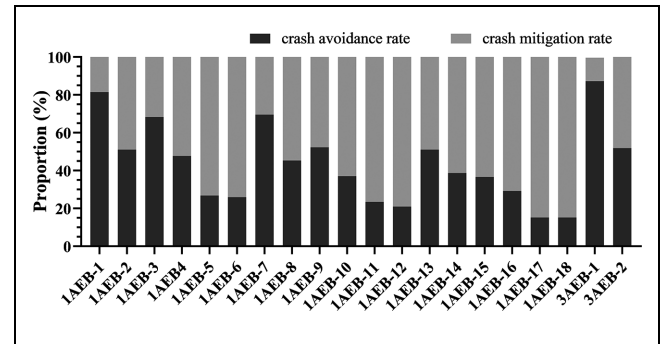
Note: the p-value in bold indicates the difference is significant.

The impact of the parameter values on the one-stage AEB crash avoidance rate was evaluated by analysis of variance (ANOVA). ANOVA revealed significant main effects of deceleration ($F_{(2,484)} = 91.80$, $p < 0.001$), TTC ($F_{(2,484)} = 177.92$, $p < 0.001$), and detection area ($F_{(2,242)} = 67.46$, $p < 0.001$) on crash avoidance rates. Post-hoc analysis tested all scenarios for the least significant difference between paired conditions (Table 3). For the 0.9 and 0.7 paired group, the average crash avoidance rate for one-stage AEB systems with a deceleration of 0.9 g is 0.088 (8.8%) higher than those with a deceleration of 0.7 g. Similarly, the average differences for the 0.9 and 0.5 and 0.7 and 0.5 paired groups are 0.192 ($p < 0.001$) and 0.104 ($p < 0.001$), respectively, showing that the crash avoidance rate is higher when a larger deceleration is applied. Higher avoidance rates were also found for one-stage AEB algorithms with larger TTC. The avoidance rate is also higher when the detection area of one-stage AEB is wide (FoV = 80°, $w = 5$ m) than when it is narrow (FoV = 40°, $w = 1$ m) ($p < 0.001$). For the three-stage AEB systems, which only differ in detection area, as is visually shown in Figure 5, the wider detection area in 3AEB-1 will lead to a significant 35.3% higher crash avoidance rate than 3AEB-2.

Crash Avoidance Rates in Different Scenarios

The crash avoidance rates for the one-stage AEB and three-stage AEB algorithms were compared for four crossing scenarios (Figure 6a) and three longitudinal scenarios (Figure 6b). Overall, the avoidance rates for crossing scenarios (mean = 35.6%) are lower than longitudinal scenarios (mean = 63.6%).

ANOVA tests of one-stage AEB revealed significant main effects of deceleration ($F_{(2,378)} = 69.610$, $p < 0.001$), TTC ($F_{(2,378)} = 119.072$, $p < 0.001$), and detection area ($F_{(2,378)} = 66.008$, $p < 0.001$) on crash avoidance rates in crossing scenarios. Post-hoc analysis in Table 3 shows

**Figure 5.** Crash avoidance and mitigation rates of one-stage and three-stage automatic emergency braking (AEB) algorithms.

that the increase of deceleration, TTC, and detection area will lead to higher avoidance rates, which is the same as the results of all types of scenarios. For longitudinal scenarios, both deceleration ($F_{(2,104)} = 22.637$, $p < 0.001$) and TTC ($F_{(2,104)} = 113.450$, $p < 0.001$) had significant main effects on the avoidance rates; however, detection area ($F_{(1,52)} = 4.016$, $p = 0.0503$) had no significant main effect. The detection area result can be vividly demonstrated by comparing the results of each pair of adjacent algorithms in Figure 6 (e.g., 1AEB-1 and 1AEB-2; 1AEB-3 and 1AEB-4), which have the same TTC and deceleration but different detection areas (refer back to Table 2). The crash avoidance rate of crossing scenarios is significantly lower when the detection area is narrow (1AEB-2 and 3AEB-2), while crash avoidance rates of longitudinal scenarios are less influenced by detection area.

Stop Distance in Avoided Crashes

For every avoided crash, the ego vehicle had stopped before the collision point. The stop distance, which is defined as the distance between the ego vehicle and the predicted collision point when the ego vehicle stopped,

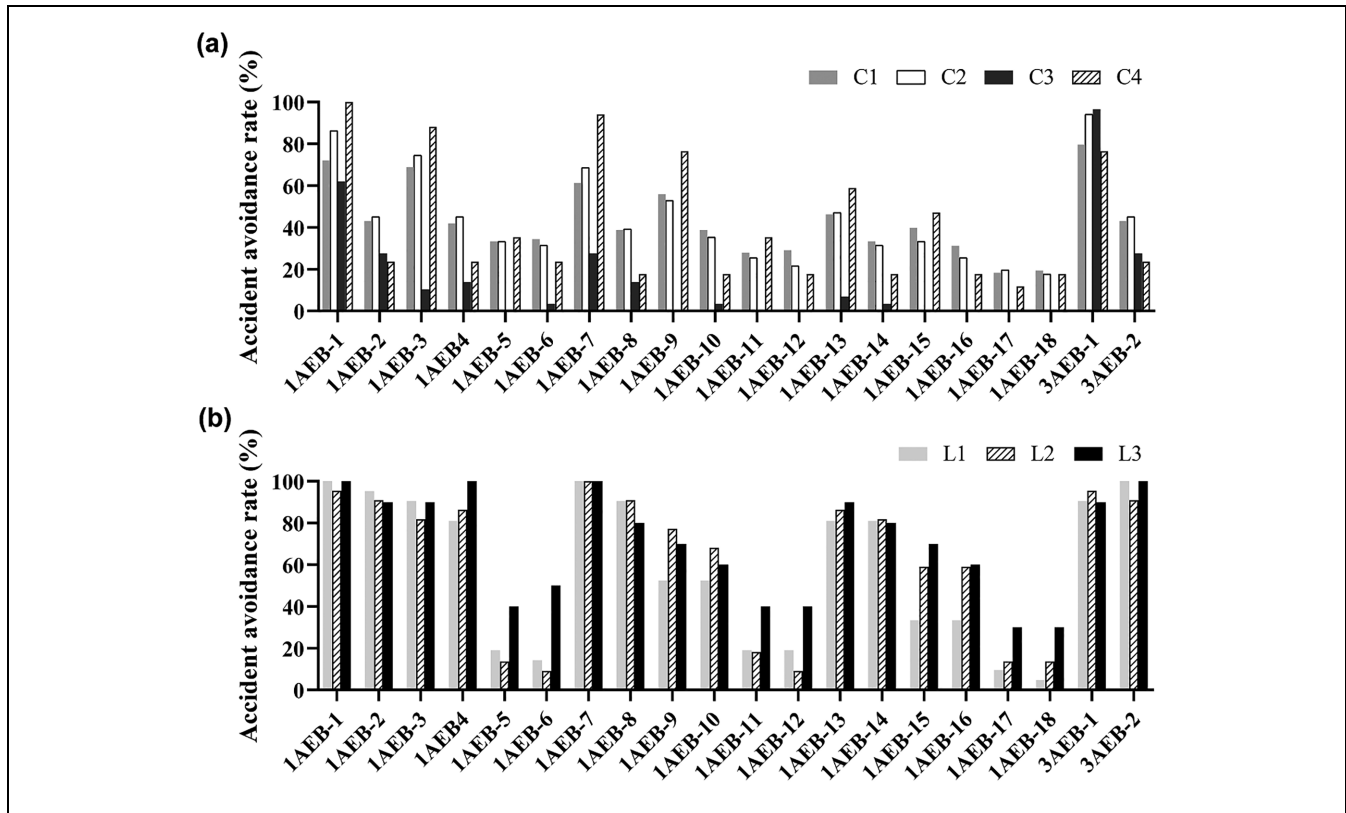


Figure 6. Crash avoidance rates for: (a) crossing scenarios and (b) longitudinal scenarios with the different automatic emergency braking (AEB) algorithms.

was calculated. The average stop distance of each AEB algorithm is plotted with its crash avoidance rate in Figure 7.

The average stop distance of one-stage AEB algorithms ranges from 0.63 m (1AEB-17) to 3.63 m (1AEB-1), while the average stop distance of 3AEB-1 and 3AEB-2 is 13.08 m and 11.4 m, respectively, significantly larger than that of one-stage AEB. As stop distance reflects the amount of road the vehicle occupies during braking, stop distance, in addition to its relationship to safety, also represents the algorithms' traffic efficiency or conservativeness. For both one-stage and three-stage AEB systems, stop distance is positively correlated with crash avoidance rate, indicating that a higher crash avoidance rate is usually accompanied by higher conservativeness and lower traffic efficiency. Though the crash avoidance of 3AEB-1 is slightly higher than that of 1AEB-1, the two three-stage AEB systems are both much more conservative than all the one-stage AEB systems, therefore resulting in lower traffic efficiency.

Speed Reduction of Severity Mitigated Crashes

For crashes that were not avoided by the AEB systems, the speed reductions were calculated to assess the degree

to which the crashes were mitigated. For each crash, the ego vehicle's collision speed was compared with its initial speed to arrive at the speed reduction. The average speed reductions of each of the AEB algorithms are shown in Figure 8a.

Average speed reduction of the one-stage AEB algorithms ranged from 6.9 km/h (1AEB-18) to 32.3 km/h (1AEB-1), all larger than the SV's average speed reduction of 5.3 km/h in the extracted crashes (refer back to Figure 1d). Comparing Figure 8a with the avoidance proportions in Figure 5, it can be seen that the speed reductions produced by the one-stage AEB algorithms follow the same trend as crash avoidance rates. To use the above example, both the speed reduction and crash avoidance rate of 1AEB-1 were the highest of the 1AEB algorithms, and those of 1AEB-18 were the lowest, indicating that the better the algorithm's collision avoidance ability, the greater its speed reduction and consequently the better its mitigation ability. On the other hand, the average speed reductions of the two three-stage AEB algorithms 3AEB-1 and 3AEB-2 are 5.80 km/h and 2.37 km/h, respectively (Figure 8a). Although Figure 5 shows that the three-stage AEB algorithms have high crash avoidance rates, their speed reductions are low, indicating that the severity of the crashes that did occur was not fully mitigated.

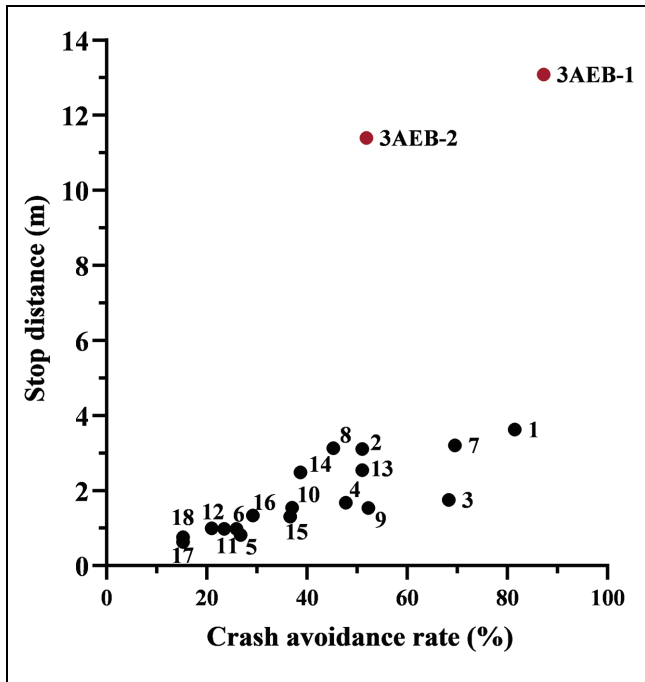


Figure 7. Stop distances and crash avoidance rates of the different automatic emergency braking (AEB) algorithms (because of limited space, one-stage AEB systems are denoted by their ID numbers 1–18 only).

To investigate why some of the crashes could not be avoided, the initial speeds of the TW and ego vehicle and their view obstruction rates were compared for crashes that were avoided and those that were only mitigated. As is shown in Figure 8b, in all the AEB algorithms except 1AEB-5 and 1AEB-11, the average initial TW speed is higher in mitigated crashes than in avoided crashes, with an average difference of 3.24 km/h. Figure 8c shows that while the three-stage AEBs show little difference, the mean initial speeds of ego vehicles for all one-stage AEB algorithms are an average of 19.36 km/h higher in mitigated crashes than in avoided crashes. It can be concluded that higher initial speeds of both ego vehicle and TW increase the likelihood of collision. For one-stage AEB systems, the influence of the speed of the ego vehicle is more significant, whereas the influence of the TW speed is more significant for three-stage AEB.

View obstruction rates of the mitigated and avoided crashes were also calculated, as common sense holds that obstructed views may lead to crashes. Figure 8d, however, shows that the view obstruction rate is much higher in avoided crashes than in mitigated crashes, indicating that view obstruction may not necessarily lead to crashes within the detection area used in this study.

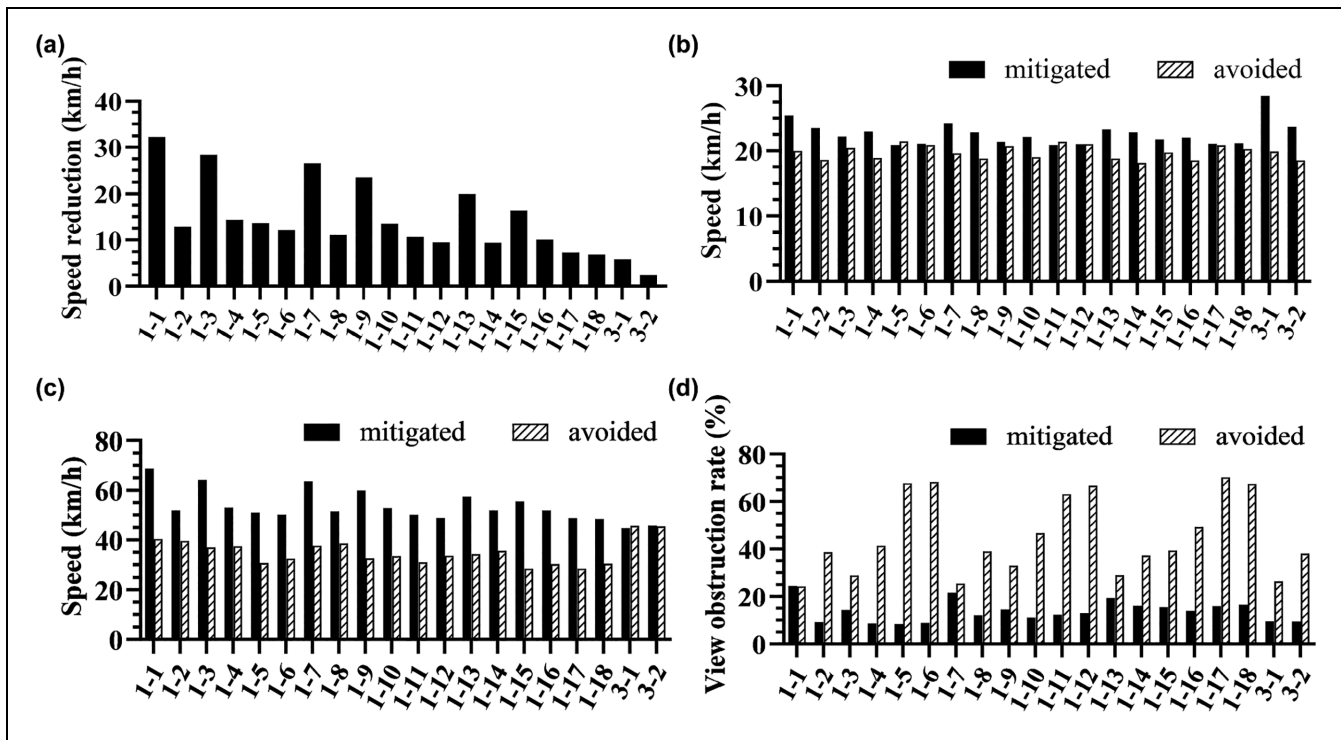


Figure 8. Analysis of mitigated and avoided crashes: (a) speed reduction, (b) initial speed of two-wheeler, (b) initial speed of ego vehicle, and (d) view obstruction rate.

Note: 1AEB-1 is denoted as 1-1, and so forth.

Discussion and Conclusion

To explore ways to ensure the safety of two-wheelers in autonomous driving environments, this study evaluated two automatic braking systems: one-stage AEB and three-stage AEB, in different crash scenarios in China. From the CIDAS database, 430 crashes were extracted and clustered into four basic types of scenarios. Crossing and longitudinal scenarios were selected for study based on their high injury severity and adequate sample sizes, resulting in a total of 243 crashes that were recreated in the Matlab simulation platform. Eighteen one-stage AEB algorithms and two three-stage AEB algorithms with different deceleration, TTC, and detection areas (FoV and trigger width) were tested with the reconstructed crashes. ANOVA was conducted on the scenarios to explore the effects of different AEB parameters on crash avoidance and mitigation rates. The correlations between crash avoidance rate and traffic efficiency, speed reduction, and TW and vehicle speed were also investigated.

The crash avoidance rate of one-stage AEB ranges from 15.2% to 81.5%, while three-stage AEB has crash avoidance rates as high as 87.2%. Algorithm 1AEB-1, with a deceleration of 0.9 g, TTC of 1.5 s, and wide detection area (FoV = 80°, $w = 5$ m), has the highest crash avoidance rate of 81.5%, which is close to the average avoidance rate of 83.6 % with FoV of 70° found in Char's study (19). ANOVA tests revealed that deceleration rate, TTC, and detection area all have significant main effects on crash avoidance rate. The AEB algorithms with large TTC and deceleration activate the brake earlier and come to a full stop faster, achieving a higher crash avoidance rate. Existing research (17, 42) has also found that large TTC and deceleration improve crash avoidance and decrease injury severity. Figure 7, however, shows that algorithms that have a high crash avoidance rate also have a large stop distance, which represents inefficient use of road resources. The Ministry of Land, Infrastructure, Transport and Tourism of Japan requires that a collision avoidance system must stop closer to the obstacle than 1 m (44), suggesting that stop distance, or more fundamentally, traffic efficiency, should be further improved in designing an AEB system. The current study found that a wide detection area (including FoV and trigger width) significantly improves the crash avoidance rate in crossing scenarios, while it has less effect on longitudinal scenarios. Similar to the results of Char et al. (19), we found that since TW riders in longitudinal scenarios are within the AV's sensor detection area most of the time, crashes that are caused by drivers' unawareness of TWs can thus be largely avoided. Moreover, a large trigger width for longitudinal scenarios may misdetect a TW in an adjacent lane as a threat. Therefore, different detection areas may be suitable for different types of scenarios. Although the FoV

size is fixed with the sensor, trigger width can be adjustable for future studies of AEB.

In the crashes that were not avoided, the AEB algorithms achieved at least an average of 2.37 km/h speed reduction, thereby mitigating the crashes. In a study by Kovaceva et al. (45) assessing the safety of cyclists and pedestrians with the German In-Depth Accident Study, crash mitigation was also evaluated by speed reduction; where all the crashes were either avoided or mitigated by speed reduction, which is consistent with our results. The current study found that one-stage AEB algorithms that have a high crash avoidance rate also have a large speed reduction. However, even though the three-stage AEB algorithms both have high crash avoidance rates, their speed reduction is low, indicating that their injury severity reduction would not be as high as one-stage AEB algorithms with similar crash avoidance rates. As three-stage AEB increases its deceleration only in correspondence with the increase of the situation's urgency (indicated by TTC), it may not be able to achieve a high deceleration as rapidly as one-stage AEB, thus resulting in lower speed reduction. Therefore, 1AEB-1 is recommended as the most effective algorithm in this study, as it has both a high avoidance rate and mitigation rate, and is also more efficient (with its shorter stop distance) than the three-stage AEB algorithms. The initial speed of the TW and ego vehicle were found to be significantly higher in crash mitigated events than in crash avoided events, but the view obstruction rate was lower in crash mitigated events than in crash avoided events. The average initial ego car velocity in view-obstructed crashes was 42.5 km/h, 4.1 km/h lower than that of crashes without obstruction, which suggests that drivers may intentionally lower their speed when the view is obstructed. As high ego vehicle speed increases the likelihood of collisions, speed, rather than view obstruction, may be the primary reason for the collisions.

This study has some limitations. Only crossing and longitudinal scenarios were tested, so the other two types of scenarios, turning and on-coming, should be studied in future research. Additionally, the simulated AV's sensor detection ability was simplified to construct ideal AEB models, so severe visibility conditions such as rain, fog, or strong change in illumination were not considered; nor were road conditions such as wet or icy pavement.

Despite these limitations, two main contributions have been made in this study. First, TW crash scenarios were clustered and analyzed, the generation process of the typical scenarios can be applied to similar simulation studies in other countries with serious TW traffic safety issues. Second, the performance of 18 one-stage and two three-stage AEB algorithms with different parameters were innovatively evaluated in different TW crash scenarios. The results not only demonstrated that AEB systems are effective in avoiding and mitigating the severity

of TW crashes, but also led to further consideration of the research concerning adjustable detection areas of AEB systems and called for deeper thoughts of balancing between safety and traffic efficiency.

Acknowledgment

The authors appreciate Barbara Rau Kyle for her helpful revision and polish.

Author Contributions

The authors confirm contribution to the paper as follows: study conception and design: W. Zhou, X. Wang; data collection: W. Zhou; analysis and interpretation of results: W. Zhou; draft manuscript preparation: W. Zhou, X. Wang. All authors reviewed the results and approved the final version of the manuscript.


Declaration of Conflicting Interests


The author(s) declared no potential conflicts of interest with respect to the research, authorship, and/or publication of this article.

Funding

The author(s) disclosed receipt of the following financial support for the research, authorship, and/or publication of this article: This study was sponsored by the National Key R&D Program of China (2021YFF0602700).

ORCID iDs

Weixuan Zhou  <https://orcid.org/0000-0002-8614-0009>

Xuesong Wang  <https://orcid.org/0000-0001-8046-3213>

References

1. The Central People's Government of the People's Republic of China. *The Number of Bicycles in China is Nearly 400 Million, Ranking First in the World*. http://www.xinhuanet.com/fortune/2019-11/22/c_1125264380.htm. Accessed February 1, 2023.
2. Traffic Management Bureau of the Public Security Ministry. *Annual Report on Traffic Accidents Statistics (Year 2019)*. Traffic Management Research Institute of the Ministry of Public Security, Wu Xi, China, 2020.
3. Department of Transport. *Reported Road Casualties in Great Britain: 2019 Annual Report*. Department of Transport, London, 2020.
4. Bureau of Infrastructure, Transport and Regional Economics (BITRE). *International Road Safety Comparisons 2019*. BITRE, Canberra, Australia, 2021.
5. Krug, E., S. Billingsley, B. Watson, and J. L. Irigoyen. *Powered Two- and Three-Wheeler Safety: A Road Safety Manual for Decision-Makers and Practitioners*. World Health Organization, Geneva, Switzerland, 2017.
6. *Road Safety Annual Report 2019 Sweden*. International Transport Forum, Paris, France, 2020.
7. Zhu, M., X. Wang, and J. Hu. Impact on Car Following Behavior of a Forward Collision Warning System with Headway Monitoring. *Transportation Research Part C: Emerging Technologies*, Vol. 111, 2020, pp. 226–244.
8. Wang, X., M. Chen, M. Zhu, and P. Tremont. Development of a Kinematic-Based Forward Collision Warning Algorithm Using an Advanced Driving Simulator. *IEEE Transactions on Intelligent Transportation Systems*, Vol. 17, No. 9, 2016, 2583–2591.
9. Fildes, B., M. Keall, N. Bos, A. Lie, Y. Page, C. Pastor, L. Pennisi, M. Rizzi, P. Thomas, C., and Tingvall. Effectiveness of Low Speed Autonomous Emergency Braking in Real-World Rear-End Crashes. *Accident Analysis & Prevention*, Vol. 81, 2015, pp. 24–29.
10. Kusano, K. D., and H. C. Gabler. Safety Benefits of Forward Collision Warning, Brake Assist, and Autonomous Braking Systems in Rear-End Collisions. *Proceedings of IEEE Transactions on Intelligent Transportation Systems*, Vol. 13, No. 4, 2012, pp. 1546–1555.
11. European Parliament, Council of the European Union. *Regulation (EU) 2019/2144 of the European Parliament and of the Council*, 2019.
12. NHTSA. *U.S. DOT and IIHS Announce Historic Commitment of 20 Automakers to Make Automatic Emergency Braking Standard on New Vehicles*. <https://www.nhtsa.gov/press-releases/us-dot-and-iihs-announce-historic-commitment-20-automakers-make-automatic-emergency-braking-standard-on-new-vehicles>. Accessed February 1, 2023.
13. Saadé, J. *Autonomous Emergency Braking AEB (Pedestrians Cyclists)*. European Road Safety Decision Support System, Loughborough, 2017.
14. Large, D. R., C. Harvey, G. Burnett, S. Leong, and J. Gabbard. Exploring the Relationship Between False Alarms and Driver Acceptance of a Pedestrian Alert System During Simulated Driving. *The Road Safety and Simulation Conference*, The Hague, The Netherlands, 2017.
15. Lee, K., and H. Peng. Evaluation of Automotive Forward Collision Warning and Collision Avoidance Algorithms. *Vehicle System Dynamics*, Vol. 43, No. 10, 2005, pp. 735–751.
16. Doecke, S. D., R. W. G. Anderson, J. Mackenzie, and G. Ponte. The Potential of Autonomous Emergency Braking Systems to Mitigate Passenger Vehicle Crashes. *Proc., Australasian Road Safety Research, Policing and Education Conference*. Wellington, New Zealand, 2012.
17. Rosen, E. Autonomous Emergency Braking for Vulnerable Road Users. *IRCOBI Conference*, Gothenburg, Sweden, 2013.
18. Lenard, J., R. Welsh, and R. Danton. Time-to-Collision Analysis of Pedestrian and Pedal-Cycle Accidents for the Development of Autonomous Emergency Braking Systems. *Accident Analysis & Prevention*, Vol. 115, 2018, pp. 128–136.
19. Char, F., T. Serre, S. Compigne, and P. Puente Guillen. Car-to-Cyclist Forward Collision Warning Effectiveness Evaluation: A Parametric Analysis on Reconstructed Real Accident Cases. *International Journal of Crashworthiness*, Vol. 27, No. 1, 2020, pp. 34–43.
20. Jeppsson, H., and N. Lubbe. Simulating Automated Emergency Braking With and Without Torricelli Vacuum Emergency Braking for Cyclists: Effect of Brake Deceleration and

- Sensor Field-of-View on Accidents, Injuries and Fatalities. *Accident Analysis & Prevention*, Vol. 142, 2020, p. 105538.
21. Peng, Y., W. Yu, X. Wang, Q. Xu, H. Wang, and W. Wu. AEB Effectiveness Research Methods Based on Reconstruction Results of Truth Vehicle-to-TW Accidents in China. *Proceedings of the Institution of Mechanical Engineers, Part D: Journal of Automobile Engineering*, Vol. 235, No. 7, 2021, pp. 2029–2039.
 22. Zhou, W., and X. Wang. Calibrating and Comparing Autonomous Braking Systems in Motorized-to-Non-Motorized-Vehicle Conflict Scenarios. *IEEE Transactions on Intelligent Transportation Systems*, Vol. 23, No. 11, 2022, pp. 20636–20651.
 23. Zhou, W., X. Wang, Y. Glaser, X. Wu, and X. Xu. Developing an Improved Automatic Preventive Braking System Based on Safety-Critical Car-Following Events from Naturalistic Driving Study Data. *Accident Analysis & Prevention*, Vol. 178, 2022, p. 106834.
 24. Wang, X., Q. Liu, F. Guo, X. Xu, and X. Chen. Causation Analysis of Crashes and Near Crashes Using Naturalistic Driving Data. *Accident Analysis & Prevention*, Vol. 177, 2022, pp. 106821.
 25. Volvo Trucks. *Towards Zero Accident with Safety Research*. <https://www.volvotrucks.com/en-en/about-us/who-we-are/our-values/safety/safety-research.html>. Accessed March 13, 2023.
 26. Federal Highway Research Institute. *Accident research - GIDAS*. https://www.bast.de/EN/Automotive_Engineering/Subjects/gidas.html. Accessed July 15, 2022.
 27. Ohlin, M., J. Strandroth, and C. Tingvall. The Combined Effect of Vehicle Frontal Design, Speed Reduction, Autonomous Emergency Braking and Helmet Use in Reducing Real Life Bicycle Injuries. *Safety Science*, Vol. 92, 2017, pp. 338–344.
 28. Sui, B., N. Lubbe, and J. Bärgman. Evaluating Automated Emergency Braking Performance in Simulated Car-to-Two-Wheeler Crashes in China: A Comparison Between C-NCAP Tests and in-Depth Crash Data. *Accident Analysis & Prevention*, Vol. 159, 2021, p. 106229.
 29. Cao, Y., L. Xiao, H. Dong, Y. Wang, X. Wu, P. Li, and Y. Qiu. Typical Pre-crash Scenarios Reconstruction for Two-Wheelers and Passenger Vehicles and Its Application in Parameter Optimization of AEB System Based on NAIS Database. *26th International Technical Conference on the Enhanced Safety of Vehicles (ESV)*, Eindhoven, Netherlands, 2019.
 30. Zhao, Y., D. Ito, and K. Mizuno. AEB Effectiveness Evaluation Based on Car-to-Cyclist Accident Reconstructions Using Video of Drive Recorder. *Traffic Injury Prevention*, Vol. 20, No. 1, 2019, pp. 100–106.
 31. Zhao, M., H. Wang, J. Chen, X. Xu, and Y. He. Method to Optimize Key Parameters and Effectiveness Evaluation of the AEB System Based on Rear-End Collision Accidents. *SAE International Journal of Passenger Cars – Electronic and Electrical Systems*, Vol. 10, 2017, pp. 310–317.
 32. Jeppsson, H., M. Östling, and N. Lubbe. Real Life Safety Benefits of Increasing Brake Deceleration in Car-to-Pedestrian Accidents: Simulation of Vacuum Emergency Braking. *Accident Analysis & Prevention*, Vol. 111, 2018, pp. 311–320.
 33. Kuehn, M., T. Hummel, and A. Lang. Cyclist-Car Accidents—Their Consequences for Cyclists and Typical Accident Scenarios. *24th International Conference on the Enhanced Safety of Vehicles*, Gothenburg, Sweden, 2015.
 34. Op den Camp, O., S. van Montfort, J. Uittenbogaard, and J. Welten. Cyclist Target and Test Setup for Evaluation of Cyclist-Autonomous Emergency Braking. *International Journal of Automotive Technology*, Vol. 18, No. 6, 2017, pp. 1085–1097.
 35. Van der Zweep, C., M. Pla, M. Wisch, T. Schaller, S. de Hair, and P. Lemmen. *Assessment Methodologies for Forward Looking Integrated Pedestrian and Further Extension to Cyclists Safety*. European Commission, Brussels, Belgium, 2014.
 36. Sui, B., N. Lubbe, and J. Bärgman. A Clustering Approach to Developing Car-to-Two-Wheeler Test Scenarios for the Assessment of Automated Emergency Braking in China Using in-Depth Chinese Crash Data. *Accident Analysis & Prevention*, Vol. 132, 2019, p. 105242.
 37. Pan, D., Y. Han, Q. Jin, H. Wu, and H. Huang. Study of Typical Electric Two-Wheelers Pre-Crash Scenarios Using K-Medoids Clustering Methodology Based on Video Recordings in China. *Accident Analysis & Prevention*, Vol. 160, 2021, p. 106320.
 38. Cicchino, J. B. Effectiveness of Forward Collision Warning and Autonomous Emergency Braking Systems in Reducing Front-to-Rear Crash Rates. *Accident Analysis & Prevention*, Vol. 99, 2016, pp. 142–152.
 39. Park, M. K., S. Y. Lee, C. K. Kwon, and S. W. Kim. Design of Pedestrian Target Selection With Funnel Map for Pedestrian AEB System. *IEEE Transactions on Vehicular Technology*, Vol. 66, No. 5, 2017, pp. 3597–3609.
 40. *Comparative Test of Advanced Emergency Braking Systems*. Allgemeiner Deutscher Automobil-Club (ADAC), Munich, Germany, 2013.
 41. *Abbreviated Injury Scale*. NSW Institute of Trauma and Injury Management, Agency for Clinical Innovation, NSW Government. https://aci.health.nsw.gov.au/networks/institute-of-trauma-and-injury-management/data/injury-scoring/abbreviated_injury_scale (accessed March 1, 2023).
 42. Chajmowicz, H., J. Saadé, and S. Cuny. Prospective Assessment of the Effectiveness of Autonomous Emergency Braking in Car-to-Cyclist Accidents in France. *Traffic Injury Prevention*, Vol. 20, 2019, pp. S20–S25.
 43. Char, F., and T. Serre. Analysis of Pre-Crash Characteristics of Passenger Car to Cyclist Accidents for the Development of Advanced Drivers Assistance Systems. *Accident Analysis & Prevention*, Vol. 136, 2020, p. 105408.
 44. Coelingh, E., A. Eidehall, and M. Bengtsson. Collision Warning With Full Auto Brake and Pedestrian Detection – a Practical Example of Automatic Emergency Braking. *13th International IEEE Conference on Intelligent Transportation Systems*, Funchal, Portugal, 2010.
 45. Kovaceva, J., A. Bálint, R. Schindler, and A. Schneider. Safety Benefit Assessment of Autonomous Emergency Braking and Steering Systems for the Protection of Cyclists and Pedestrians Based on a Combination of Computer Simulation and Real-World Test Results. *Accident Analysis & Prevention*, Vol. 136, 2020, p. 105352.